

## Macrocycle Topology

## Aggregation-Induced-Emission-Active Macrocycle Exhibiting Analogous Triply and Singly Twisted Möbius Topologies

Erjing Wang,<sup>[a, b, c]</sup> Zikai He,<sup>[a, b]</sup> Engui Zhao,<sup>[a, b]</sup> Luming Meng,<sup>[b]</sup> Christian Schütt,<sup>[d]</sup> Jacky W. Y. Lam,<sup>[a, b]</sup> Herman H. Y. Sung,<sup>[b]</sup> Ian D. Williams,<sup>[b]</sup> Xuhui Huang,<sup>[b]</sup> Rainer Herges,<sup>\*,[d]</sup> and Ben Zhong Tang<sup>\*,[a, b, e]</sup>

**Abstract:** Molecules with Möbius topology have drawn increasing attention from scientists in a variety of fields, such as organic chemistry, inorganic chemistry, and material science. However, synthetic difficulties and the lack of functionality impede their fundamental understanding and practical applications. Here, we report the facile synthesis of an aggregation-induced-emission (AIE)-active macrocycle (TPE-ET) and investigate its analogous triply and singly twisted Möbius topologies. Because of the twisted and flexible nature of the tetraphenylethene units, the macrocycle adjusts its conformations so as to accommodate different guest molecules in its crystals. Moreover, theoretical studies including topological and electronic calculations reveal the energetically favorable interconversion process between triply and singly twisted topologies.

Molecules with intriguing topologies stimulate the imagination of scientists because of their (theoretically predicted) unusual

properties as well as the challenges involved in their synthesis.<sup>[1]</sup> Just like other molecular topologies, such as catenanes, rotaxanes, and knots, non-orientable Möbius bands have aroused wide interest from synthetic chemists.<sup>[2]</sup> Continuous efforts devoted to the synthesis of Möbius-type molecules notwithstanding,<sup>[3]</sup> it was not until 2003 that the first stable Möbius hydrocarbon was prepared by Herges et al.<sup>[4]</sup> The difficulty in the synthesis of Möbius-type molecules is mainly due to the high strain caused by the twist.<sup>[5]</sup> Consequently, the synthesis of multiply twisted Möbius macrocycles should be even more difficult owing to increased strain.<sup>[6]</sup>

In topological analysis, three parameters, linking number ( $L_k$ ), twist ( $T_w$ ), and writhe ( $W_r$ ), are applied to define the geometry of a closed twisted ribbon. The three parameters are connected by the Călugăreanu theorem as:  $L_k = W_r + T_w$ .<sup>[7]</sup> The linking number  $L_k$  is an integer, with even numbers of  $L_k$  describing orientable and two-sided ribbons, whereas odd numbers of  $L_k$  denote non-orientable and one-sided ribbons, such as Möbius systems. Generally, a closed ribbon with a higher order of  $L_k$  tends to release its strain by projecting twist into writhe. Rzepa<sup>[8]</sup> and Herges<sup>[9]</sup> proposed to apply this feature to construct annulenes with higher Möbius topologies. Guided by this strategy, the first triply Möbius dehydroannulene ( $L_k = 3$ ) was successfully prepared in 2014.<sup>[10]</sup> As shown in Figure 1, the

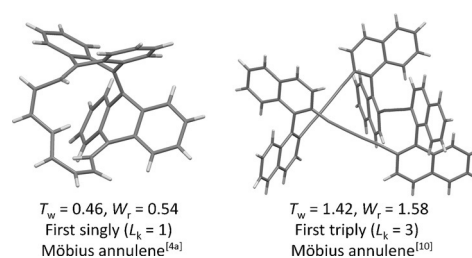


Figure 1. Structures of the first singly and triply Möbius hydrocarbons.

macrocycle is only slightly strained ( $T_w = 1.42$ ) because most of the twist is transformed into writhe through the chiral 1,1'-binaphthyl units. Another interesting feature of molecular Möbius bands is their ability to change the degree of twist through topology flipping. However, to date, most reported Möbius systems have been made deliberately rigid to stabilize the twisted conformation, with a few expanded porphyrins examples exhibiting reversible switching between different topologies.<sup>[11]</sup>

[a] E. Wang,<sup>+</sup> Z. He,<sup>+</sup> E. Zhao, J. W. Y. Lam, Prof. B. Z. Tang  
HKUST Shenzhen Research Institute, No. 9 Yuexing 1st RD  
South Area, Hi-tech Park Nanshan, Shenzhen 518057 (China)  
E-mail: tangbenz@ust.hk

[b] E. Wang,<sup>+</sup> Z. He,<sup>+</sup> E. Zhao, L. Meng, J. W. Y. Lam, H. H. Y. Sung,  
Prof. Dr. I. D. Williams, Prof. X. Huang, Prof. B. Z. Tang  
Department of Chemistry, Division of Life Science  
State Key Laboratory of Molecular Neuroscience  
Institute for Advanced Study  
Institute of Molecular Functional Materials  
Division of Biomedical Engineering  
The Hong Kong University of Science and Technology  
Clear Water Bay, Kowloon, Hong Kong (China)

[c] E. Wang<sup>+</sup>  
School of Materials Science and Engineering, Hubei University  
No. 368, Youyi Avenue, Wuhan 430062 (China)

[d] C. Schütt, Prof. R. Herges  
Institute for Organic Chemistry, University of Kiel  
Otto-Hahn-Platz 4, 24098 Kiel (Germany) iso-kiel.de  
E-mail: rherges@oc.uni-kiel.de

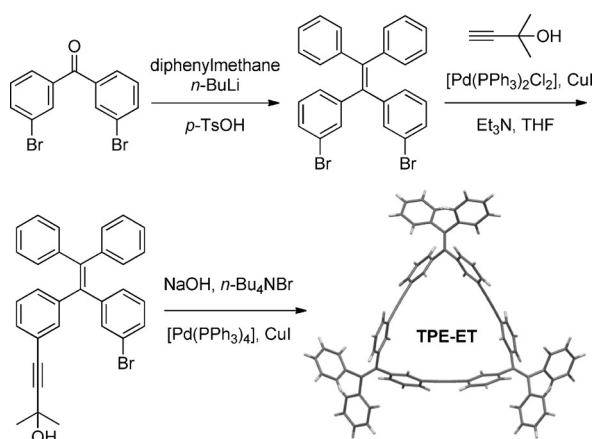
[e] Prof. B. Z. Tang  
Joint Research Laboratory  
State Key Laboratory of Luminescent Materials and Devices  
South China University of Technology  
Guangzhou 510640 (China)

[<sup>+</sup>] Both authors contributed equally to this work.

Supporting information for this article is available on the WWW under  
<http://dx.doi.org/10.1002/chem.201502224>.

To design high-order Möbius molecules with switchable topologies, two factors need to be considered: a well-defined chiral “writhe precursor” to release the strain in the Möbius structure and a relatively flexible conformation to allow topology flipping. These properties are met by tetraphenylethene (TPE), which exhibits novel aggregation-induced emission (AIE) owing to the propeller-like structure and which has recently been extensively applied in chemo/biosensors.<sup>[12]</sup> The intrinsic turn generated by the adjacent phenyl rings and their free rotational motion with respect to the central double bond make TPEs excellent candidates for the construction of switchable Möbius rings. However, to the best of our knowledge, utilizing TPE units to construct multiply Möbius topologies remains unexplored, despite the considerable research interest in constructing macrocycles with TPE motifs.<sup>[13,14]</sup> Herein, we report the first example of a TPE-containing ring (TPE-ET), which exhibits analogously singly and triply twisted Möbius topologies, as well as AIE characteristics.

The structure and synthetic route to TPE-ET are shown in Scheme 1. A one-step modified Sonogashira coupling of an in situ deprotected monomer led to the cyclization, yielding the trimeric macrocycle TPE-ET. The isolated yield is 10%, which



**Scheme 1.** Synthesis of the TPE-ET macrocycle.

corresponds to a yield of 47% for each coupling including in situ deprotection. It is lower than reported examples,<sup>[15]</sup> but the synthesis is much more straightforward and easier compared with the first triply Möbius dehydroannulene.<sup>[10]</sup> TPE-ET has moderate solubility in common organic solvents, such as dichloromethane, chloroform, THF, and acetone. The structure was fully characterized by <sup>1</sup>H NMR and <sup>13</sup>C NMR spectroscopy, as well as high-resolution mass spectrometry (Figures S1 and S2 in the Supporting Information).

We then investigated the photophysical properties of TPE-ET and its building unit, 3,3'-(2,2-diphenylethene-1,1-diyl)bis(ethylbenzene) (TPEyne, Scheme S1 in the Supporting Information). As shown in Figure S3 (see the Supporting Information), TPE-ET exhibits a blueshifted absorption maximum compared with TPEyne, indicating the higher degree of twisting in TPE-ET. Moreover, TPE-ET also exhibits typical AIE characteristics. It

is almost non-emissive in homogeneous solutions of THF and highly emissive when it forms aggregates in THF/water mixtures that have water fractions higher than 90% (Figure S4 in the Supporting Information). Similar properties are observed for TPEyne (Figure S5 in the Supporting Information). The emission peak of TPE-ET in the aggregated state is located at 457 nm, which is 20 nm blueshifted compared with TPEyne, verifying that the cyclization rigidifies and twists the conformation of the TPE units. The AIE properties should originate from the well-known restriction of intramolecular rotation process.<sup>[12b]</sup> The excited states in solution decay through nonradiative pathways through rotations of the phenyl groups. Upon aggregation, these intramolecular rotations are suppressed. Thus, the radiative decay pathway is populated. The AIE characteristics also reveal the flexible nature of the TPE-ET structure.

As a propeller-shaped molecule, when twisting in one direction, achiral TPE can take two chiral conformations (*P* or *M* as shown in Figure 2).<sup>[16]</sup> In solution, they exist as a racemate due

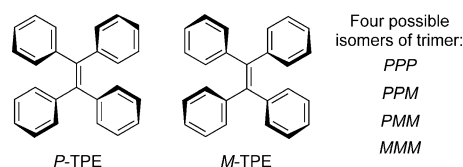


**Figure 2.** Structures of the two chiral TPE conformations and their four possible combinations in the trimeric macrocycle.

to the fast interconversion. However, in the crystalline state, the molecular conformation is fixed and can be easily determined by X-ray diffraction analysis. Two kinds of crystals of TPE-ET suitable for X-ray crystallography were obtained from CHCl<sub>3</sub>/cyclohexane (**C-1**) and CHCl<sub>3</sub>/*n*-hexane (**C-2**) solutions through slow evaporation. As shown in Figure 3, most of the crystals prepared from CHCl<sub>3</sub>/cyclohexane are hexagonal or prism-like, whereas those obtained from CHCl<sub>3</sub>/*n*-hexane are rod-like. We also tried to grow crystals of TPE-ET in CHCl<sub>3</sub>/*n*-hexane/cyclohexane. It turned out that the same crystal structure as **C-1** was obtained, indicating that the TPE-ET macrocy-

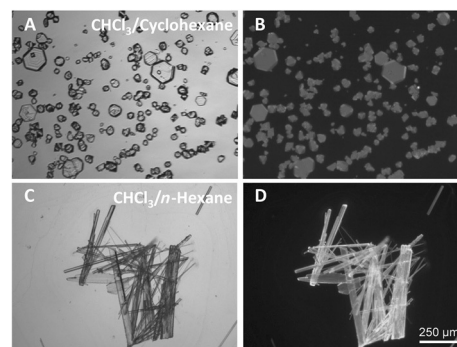


**Figure 3.** Images of TPE-ET crystals grown from CHCl<sub>3</sub>/cyclohexane and CHCl<sub>3</sub>/*n*-hexane (A, C under bright field; B, D under UV-light irradiation; wavelength: 330–380 nm; scale bar: 250 μm).

cle of **C-1** should be the thermodynamically more stable of the two. Both types of crystals emit blue light under UV irradiation in agreement with the AIE properties.

X-ray crystallography analysis revealed that both crystals trap solvent molecules because of the intrinsic cavity of the macrocycle and the nano-sized porous crystal structure. As shown in Figure 4A, two cyclohexane molecules with chair conformation are encapsulated in the center of the TPE-ET macrocycle with coinciding  $C_3$  axes of cyclohexane and **C-1**. In **C-2**, however, one *n*-hexane molecule with staggered conformation stands in the macrocyclic cavity, while another *n*-hexane molecule is surrounded by two TPE units with some disorder (Figure 4B). In addition, one chloroform molecule is trapped in the nano-sized pore of **C-2** through strong CH to  $\pi$  interactions (2.545 Å).

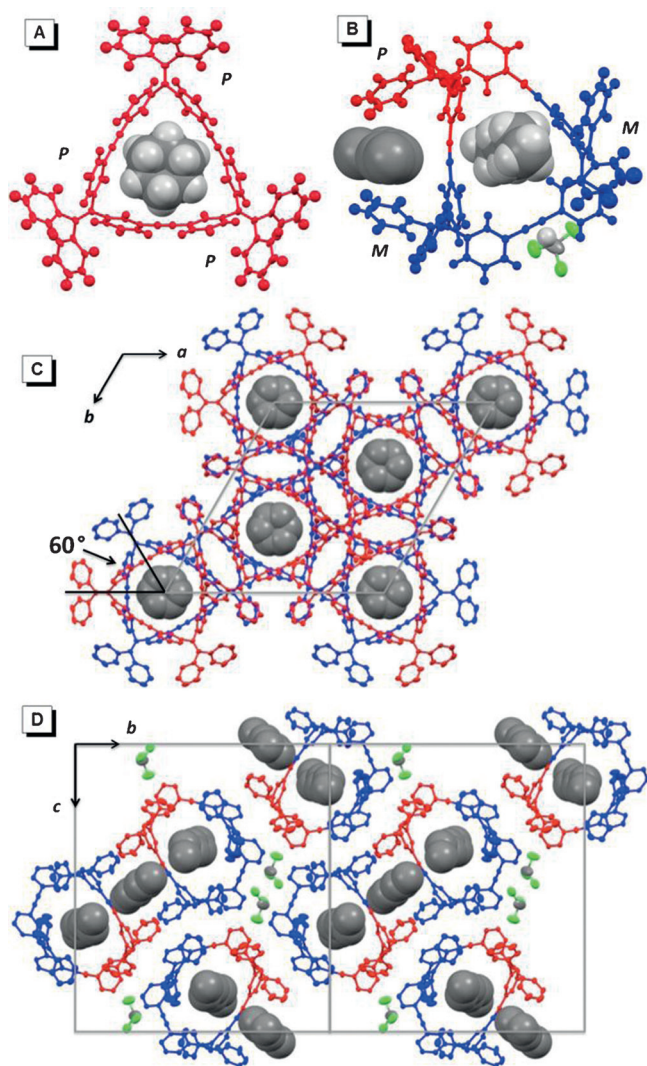


**Figure 4.** Single-crystal X-ray structures of **C-1** and **C-2**. (A)–(B) Top view showing that solvent molecules are included in macrocycle cavities and outside channels. (C) Molecular packing of **C-1** viewed along the *c* axis. (D) Molecular packing of **C-2** viewed along the *a* axis. Cyclohexane and *n*-hexane molecules are drawn as space filling models, other atoms are shown as 50% probability ellipsoids. The *P* enantiomer of the TPE unit is shown in red, the *M* enantiomer is shown in blue. Other carbon, chlorine and hydrogen atoms are shown in gray, green and white, respectively.

Interestingly, the TPE-ET macrocycle adopts suitable conformations so as to accommodate solvent molecules with different shapes and sizes. In the **C-1** crystal, it takes on a *PPP* or *MMM* configuration with  $D_3$  symmetry, whereas in the **C-2** crystal a *PMM* or *MPP* conformation with quasi- $C_2$  symmetry is preferred. In the crystal of **C-1**, the TPE-ET macrocycles in *PPP* and *MMM* configuration stack layer by layer in alternating sequence, in a coaxial manner with a perpendicular rotation angle of  $60^\circ$  (Figure 4C). This type of packing generates hexagonal channels, which are filled perfectly by cyclohexane molecules in chair conformation. The packing is stabilized by three CH to  $\pi$  interactions (2.884 Å) between cyclohexane and the carbon–carbon triple bonds. In the crystal of **C-2**, TPE-ET adopting *PMM* conformation mainly forms two kinds of channels (Figure 4D). The channels formed by the macrocycle cavities are filled by *n*-hexane molecules in staggered conformation, whereas the channels constructed by four adjacent TPE units with *PMPM* conformation are filled by *n*-hexane molecules with some disorder.

The X-ray crystallography analysis revealed the analogous Möbius topology of TPE-ET macrocycle. To check the Möbius topological nature of the macrocycle, we can either examine the structure-based definition or check its Möbius topology. The structure-based definition relies on counting the *transoid* units (the sum of all *trans* C=C bonds and *s-trans* C–C bonds),<sup>[17]</sup> which is not suitable for TPE-ET as it is neither annulene nor dehydroannulene. Therefore, taking the  $\pi$  system as a band, we construct a band orthogonal to the  $\pi$  system and cut it down in the middle (Figure S8 in the Supporting Information).<sup>[10]</sup> A trefoil knot is obtained from *PPP* Möbius topology, with a linking number of 3 (Figure 5B<sup>[18]</sup>). In contrast, one ring (double the diameter) is obtained from *PMM* Möbius topology, with a linking number of 1 (Figure 5D<sup>[18]</sup>). The Möbius feature was further verified by density functional theory (DFT) calculations (on B3LYP/6-31G(d,p) basis set). To directly visualize the Möbius topology, molecular orbitals lower than the HOMO were examined, owing to their fewer nodes, which may

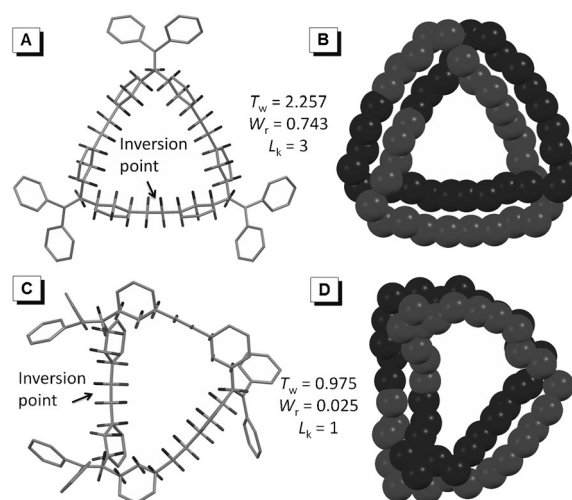


**Figure 5.** Topological diagrams to investigate the linking number  $L_k$  of the  $\pi$  system.



present Möbius topology in a much clearer way. The calculated frontier orbitals clearly show a triply twisted topology for *PPP* conformation and a singly twisted topology for *PPM* conformation in the HOMO–3 orbital (Figure S9 in the Supporting Information), corroborating the Möbius topological nature of these conformations.

The Möbius-analogous property of TPE-ET was further investigated by using the program ANEWRITHM (F. Köhler, University of Kiel).<sup>[19]</sup> Linking numbers of 3 and 1 were determined for the *PPP* conformation in **C-1** and the *PMM* conformation in **C-2**, respectively, (enantiomers have linking numbers of opposite sign). The results are consistent with their Möbius properties and the DFT calculation results discussed above. The high twist and low writhe values ( $T_w=2.257$ ,  $W_r=0.743$  in **C-1** and  $T_w=0.975$ ,  $W_r=0.025$  in **C-2**) reveal that only a relative small fraction of twist is projected into writhe. The ten times larger  $W_r$  proportion in the *PPP* conformation indicates its smaller torsion and lower strain. The more extended structure of **C-1** is also supported by UV/Vis and photoluminescent (PL) spectra (Figures S6 and S7 in the Supporting Information). The UV/Vis absorption maxima of TPE-ET in **C-1** form, **C-2** form, and in solution are 311, 309, and 307 nm, respectively, whereas the corresponding emission maxima are 466, 462, and 463 nm. These results indicate that TPE-ET in **C-1** form, with its triply twisted system, is less strained, exhibiting redshifted absorption and emission peaks.

The flexible nature of TPE-ET permits the transformation between different conformations. With the aid of theoretical calculations, we estimated the feasibility of the interconversion between *PPP* and *PPM* (or *MMM* and *PMM*) at the B3LYP/6-31G level. The energy difference between *PPP* and *PPM* was 0.75 kcal mol<sup>-1</sup> and energy barrier for the flipping was calculated to be 8.49 kcal mol<sup>-1</sup> lower than stepwise rotation of the three related dihedral angles (Figures S11 and S12 in the Supporting Information). The fact that two kinds of crystals were obtained at room temperature also indicates such a facile transformation. Therefore, the two intriguing Möbius topologies are sufficiently flexible to switch. The intrinsic twist and the flexible nature of the TPE unit should play a key role in the conformation flipping between the two Möbius topologies.

In conclusion, a novel AIE-active macrocycle, TPE-ET, was synthesized through a simple one-step modified Sonogashira cyclization. The macrocycle adjusts its conformation to accommodate different guest molecules with different shapes and sizes in related crystalline supramolecular grids, resulting in intriguing analogous triply and singly twisted Möbius topologies. DFT calculations reveal that the interconversion of these conformations is energetically favorable. This work may provide instructions for the design of novel Möbius molecular topologies and open new access to the design of novel chemo/biosensors.

## Acknowledgements

This work was partially supported by National Basic Research Program of China (973 Program; 2013CB834701), the Research

Grants Council of Hong Kong (604913, 16301614, and N\_HKUST604/14), and the University Grants Committee of Hong Kong (AoE/P-03/08). B.Z.T. thanks the support from Guangdong Innovative Research Team Program (201101C0105067115).

**Keywords:** aggregation-induced emission • macrocycles • möbius topology • topology flipping

- [1] a) H. L. Frisch, E. Wasserman, *J. Am. Chem. Soc.* **1961**, *83*, 3789–3795; b) C. A. Schalley, *Angew. Chem. Int. Ed.* **2004**, *43*, 4399–4401; *Angew. Chem.* **2004**, *116*, 4499–4501; c) R. S. Forgan, J.-P. Sauvage, J. F. Stoddart, *Chem. Rev.* **2011**, *111*, 5434–5464.
- [2] *History of Topology* (Ed. I. M. James), Elsevier, Amsterdam, **1999**, 909–924.
- [3] a) R. Herges, *Chem. Rev.* **2006**, *106*, 4820–4842; b) H. S. Rzepa, *Chem. Rev.* **2005**, *105*, 3697–3715; c) T. Kawase, M. Oda, *Angew. Chem. Int. Ed.* **2004**, *43*, 4396–4398; *Angew. Chem.* **2004**, *116*, 4496–4498.
- [4] a) D. Ajami, O. Oeckler, A. Simon, R. Herges, *Nature* **2003**, *426*, 819–821; b) C. Castro, Z. Chen, C. S. Wannere, H. Jiao, W. L. Karney, M. Mauksch, R. Puchta, N. J. R. v. E. Hommes, P. v. R. Schleyer, *J. Am. Chem. Soc.* **2005**, *127*, 2425–2432; c) S. Taubert, D. Sundholm, F. Pichierri, *J. Org. Chem.* **2009**, *74*, 6495–6502.
- [5] a) Z. S. Yoon, A. Osuka, D. Kim, *Nat. Chem.* **2009**, *1*, 113–122; b) M. Stępień, L. Latos-Grażyński, N. Sprutta, P. Chwalisz, L. Szterenber, *Angew. Chem. Int. Ed.* **2007**, *46*, 7869–7873; *Angew. Chem.* **2007**, *119*, 8015–8019; c) T. Yoneda, Y. M. Sung, J. M. Lim, D. Kim, A. Osuka, *Angew. Chem. Int. Ed.* **2014**, *53*, 13169–13173; *Angew. Chem.* **2014**, *126*, 13385–13389; d) Y. Tanaka, S. Saito, S. Mori, N. Aratani, H. Shinokubo, N. Shibata, Y. Higuchi, Z. S. Yoon, K. S. Kim, S. B. Noh, J. K. Park, D. Kim, A. Osuka, *Angew. Chem. Int. Ed.* **2008**, *47*, 681–684; *Angew. Chem.* **2008**, *120*, 693–696; e) J.-Y. Shin, K. S. Kim, M.-C. Yoon, J. M. Lim, Z. S. Yoon, A. Osuka, D. Kim, *Chem. Soc. Rev.* **2010**, *39*, 2751–2767.
- [6] C. S. Wannere, H. S. Rzepa, B. C. Rinderspacher, A. Paul, C. S. M. Allan, H. F. Schaefer III, P. v. R. Schleyer, *J. Phys. Chem. A* **2009**, *113*, 11619–11629.
- [7] G. Călugăreanu, *Czech. Math. J.* **1961**, *11*, 588–625.
- [8] S. Rappaport, H. S. Rzepa, *J. Am. Chem. Soc.* **2008**, *130*, 7613–7619.
- [9] G. R. Schaller, R. Herges, *Chem. Commun.* **2013**, *49*, 1254–1260.
- [10] G. R. Schaller, F. Topic, K. Rissanen, Y. Okamoto, J. Shen, R. Herges, *Nat. Chem.* **2014**, *6*, 608–613.
- [11] Examples of Möbius topologies flipping: a) M. Stępień, B. Szyszko, L. Latos-Grażyński, *J. Am. Chem. Soc.* **2010**, *132*, 3140–3152; b) M. Alonso, P. Geerlings, F. De Proft, *Chem. Eur. J.* **2013**, *19*, 1617–1628; c) E. Pacholska-Dudziak, J. Skonieczny, M. Pawlicki, L. Szterenber, Z. Ciunik, L. Latos-Grażyński, *J. Am. Chem. Soc.* **2008**, *130*, 6182–6195; d) J. M. Lim, M. Inoue, Y. M. Sung, M. Suzuki, T. Higashino, A. Osuka, D. Kim, *Chem. Commun.* **2011**, *47*, 3960–3962; e) M. Stępień, N. Sprutta, L. Latos-Grażyński, *Angew. Chem. Int. Ed.* **2011**, *50*, 4288–4340; *Angew. Chem.* **2011**, *123*, 4376–4430.
- [12] a) J. Luo, Z. Xie, J. W. Y. Lam, L. Cheng, C. Qiu, H. S. Kwok, X. Zhan, Y. Liu, D. Zhu, B. Z. Tang, *Chem. Commun.* **2001**, 1740–1741; b) J. Mei, Y. Hong, J. W. Y. Lam, A. Qin, Y. Tang, B. Z. Tang, *Adv. Mater.* **2014**, *26*, 5429–5479; c) Y. Yuan, R. T. K. Kwok, B. Z. Tang, B. Liu, *J. Am. Chem. Soc.* **2014**, *136*, 2546–2554; d) Y. Hong, J. W. Y. Lam, B. Z. Tang, *Chem. Soc. Rev.* **2011**, *40*, 5361–5388; e) D. Ding, K. Li, B. Liu, B. Z. Tang, *Acc. Chem. Res.* **2013**, *46*, 2441–2453.
- [13] a) H.-T. Feng, Y.-S. Zheng, *Chem. Eur. J.* **2014**, *20*, 195–201; b) J.-H. Wang, H.-T. Feng, J. Luo, Y.-S. Zheng, *J. Org. Chem.* **2014**, *79*, 5746–5751; c) S. Song, Y.-S. Zheng, *Org. Lett.* **2013**, *15*, 820–823; d) S. Song, H.-F. Zheng, H.-T. Feng, Y.-S. Zheng, *Chem. Commun.* **2014**, *50*, 15212–15215; e) M. V. R. Raju, H.-C. Lin, *Org. Lett.* **2014**, *16*, 5564–5567.
- [14] Examples of arene-ethynyl macrocycles: a) J. M. W. Chan, J. R. Tischler, S. E. Kooi, V. Bulovic, T. M. Swager, *J. Am. Chem. Soc.* **2009**, *131*, 5659–5666; b) B. Esser, F. Rominger, R. Gleiter, *J. Am. Chem. Soc.* **2008**, *130*, 6716–6717; c) B. L. Merner, L. N. Dawe, G. J. Bodwell, *Angew. Chem. Int. Ed.* **2009**, *48*, 5487–5491; *Angew. Chem.* **2009**, *121*, 5595–5599.
- [15] Z. He, X. Xu, X. Zheng, T. Ming, Q. Miao, *Chem. Sci.* **2013**, *4*, 4525–4531.

- [16] a) K. Tanaka, D. Fujimoto, T. Oeser, H. Irngartinger, F. Toda, *Chem. Commun.* **2000**, 413–414; b) K. Maeda, Y. Okamoto, N. Morlender, N. Haddad, I. Eventova, S. E. Biali, Z. Rappoport, *J. Am. Chem. Soc.* **1995**, *117*, 9686–9689.
- [17] C. Castro, W. L. Karney, *J. Phys. Org. Chem.* **2012**, *25*, 612–619.
- [18] Color versions can be found in the Supporting Information.
- [19] K. Klenin, J. Langowski, *Biopolymers* **2000**, *54*, 307–317.

---

Received: June 7, 2015

Published online on July 14, 2015

---